JOURNAL OF MECHANICS OF CONTINUA AND MATHEMATICAL SCIENCES
www.journalimcms.org

ISSN (Online) : 2454 -7190 Vol.-18, No.-02, February (2023) pp 20-44 ISSN (Print) 0973-8975

SIMULATION OF WAVE SOLUTIONS OF A FRACTIONAL-ORDER BIOLOGICAL POPULATION MODEL

Md. Sabur Uddin[1], Md. Nur Alam[2], Kanak Chandra Roy[3]

[1,3] Department of Applied Mathematics, Gono Bishwabidyalay, Savar, Dhaka, Bangladesh.

[2] Department of Mathematics, Pabna University of Science & Technology, Pabna-6600, Bangladesh.

Email: [1]bd.sabur12@gmail.com, [2]nuralam.pstu23@gmail.com, nuralam23@pust.ac.bd, [3]kanak_gb@yahoo.com

https://doi.org/10.26782/jmcms.2023.02.00002

(Received: November 10, 2022; Accepted: January 28, 2023)

Abstract

In this analysis, we apply prominent mathematical systems like the modified (G'/G)-expansion method and the variation of (G'/G)-expansion method to the nonlinear fractional-order biological population model. We formulate twenty-three mathematical solutions, which are clarified hyperbolic, trigonometric, and rational. Using MATLAB software, we illustrate two-dimensional, three-dimensional, and contour shapes of our obtained solutions. These mathematical systems depict and display its considerate and understandable technique that generates a king type shape, singular king shapes, soliton solutions, singular lump and multiple lump shapes, periodic lump and rouge, the intersection of king and lump wave profile, and the intersection of lump and rogue wave profile. Measuring our return and that gained in the past released research shows the novelty of our analysis. These systems are also capable to represents various solutions for other fractional models in the field of applied mathematics, physics, and engineering.

Keywords: Nonlinear fractional order biological model, the modified (G'/G)-expansion method, the variation of (G'/G)-expansion method, mathematical solutions, nonlinear partial differential equations, lump, and rogue wave.

I. Introduction

Nonlinear fractional order biological population model (NFBPM) are widely executed to communicate plenty of substantial miracles and nonlinear dynamical implementations in the field of applied mathematics, mathematical physics, engineering, image processing, biology, stochastic dynamical systems and others related fields. For obtaining the exact solutions of NFBPMs, numerous effective and good setup approaches have been demonstrated including the variation of (G'/G)-

expansion method [XXII], modified (G'/G)-expansion schemes [XXV, XXIV, XXVI, XXIII], fractional sub-equation technique [XV,XXIX], Sine-Gordon expansion method [IV], Kudryashov schemes [XVIII], Jacobi elliptic task technique [XIX], the Jacobi elliptic ansatz technique [VIII], fractional iteration algorithm [XIII, XIV], the unified technique [XXVII], modified decomposition schemes [III], the hyperbolic and exponential ansatz method [VII], natural transformation technique [XII], Hirota's simple schemes [XX, XVII], the modified extended tanh expansion system [VI], and significantly more. At present, Shehata and Amra [V] found a significantly critical growth of the (G'/G)- expansion process, called the variation of (G'/G) -expansion development strategy to get exact solutions of fractional nonlinear biological population models. We instrument the variation of (G'/G)-expansion way and modified (G'/G)-expansion schemes for making exact solutions to the fractional nonlinear models in the current work to communicate the reasonable and straightforwardness of the cycle. Thusly, we can easily trade the partial request nonlinear populace models into NPDE or NODE through fitting transformation, for the reason everyone familiar with fragmentary analytics comes up short on any difficulty. The main benefit of the cycle executed in this concentrate over different plans is that it contributes extra novel exact solutions, including added independent parameters, and we make a couple of novel outcomes too. The specific responses have a huge importance in revealing the principal gadget of the actual occasions. Aside from the powerful importance, the specific responses of fractional order nonlinear population models support the mathematical solvers to analyze their outcomes' precision and help them in solidness examination. In our ongoing exertion, we instrument the variation of (G'/G) - expansion scheme and modified (G'/G)-expansion scheme for developing exact solutions of NFBPM. We can consequently effectively change over NFBPM into nonlinear PDE or ODE by means of fitting transformation, with the motivation behind everyone familiar with fractional math coming up short on any difficulty.

In this stream object, the first segment presents the option of the investigation as an introduction. The second segment represents several investigations of the variation of (G'/G) - expansion scheme and modified (G'/G)-expansion scheme. In the third segment, we will get the solutions of the NFBPM equation through the considered technique. In the fourth segment, we will deliver numerous computative simulations of the solution obtained. The conclusion is presented in the last segment.

II. Methodology and fractional calculus

In this section of the analysis, overall instructions on fractional calculus theory can be found at [XXI, I, XVI]. In this paper, we will use the modified (G'/G)-expansion and variation of (G'/G)-expansion methods [XXVIII, XXX, II, IX] to solve nonlinear fractional partial differential equations in the sense of modified Riemann-Liouvalle derivative by Jumarie [X]. The Jumarie's modified Riemann-Liouvalle derivative of order γ is defined by the following expression :

$$D_t^{\gamma} f(t) = \begin{cases} \frac{1}{\Gamma(1-\gamma)} \frac{d}{dt} \int_0^t (t-\Xi)^{-\gamma} (f(\Xi) - f(0)) d\Xi, \\ 0 < \gamma \le 1, \\ (f^{(n)}(t))^{(n-\alpha),} \\ n \le \gamma < n+1, \; n \ge 1. \end{cases} \tag{1}$$

Some important properties of the fractional modified Riemann-Liouvalle derivative have been summarized and some useful formulas of them are [XI]

$$D_t^{\gamma} t^r = \frac{\Gamma(1+r)}{\Gamma(1+r-\gamma)} t^{r-\gamma}, \tag{2}$$

$$D_t^{\gamma} (f(t)g(t)) = g(t) D_t^{\gamma} f(t) + f(t) D_t^{\gamma} g(t), \tag{3}$$

$$D_t^{\gamma} f[g(t)] = f_g{}' [g(t)] D_t^{\gamma} g(t) = D_g^{\gamma} [g(t)] (g'(t))^{\gamma}. \tag{4}$$

We consider

$$T(Q, Q_x, Q_{xx}, Q_y, Q_{yy}, Q_t, Q_{tt}, Q_{xy}, Q_{xt}, Q_{yt} ...) = 0, \tag{5}$$

Where T is a polynomial of Q as well as its derivatives. In this equation, the partial fractional derivatives involving the highest order derivatives and the nonlinear terms are included. Le and He [31, 32] proposed a fractional complex transform to convert fractional differential equations into ordinary differential equations (ODE).

Implement the traveling variable:

$$Q = Q(x, y, t) = Q(\Xi), \; \Xi = p_3 \left(x + iy - \frac{a t^{\gamma}}{\Gamma(1+\gamma)} \right), \tag{6}$$

where p_3 and a are a constant to be determined later. Implementing (6) into (5), we find:

$$S\left(Q, p_3 Q', p_3^2 Q'', -p_3 a\, Q', .- p_3^2\, a^2 Q'', ...\right) = 0. \tag{7}$$

II.i. The modified (G'/G)-expansion method

According to the modified (G'/G)-expansion method, we have

$$Q(\Xi) = \sum_{i=-S}^{S} V_i \Delta^i, \tag{8}$$

where $\Delta = \left(\frac{G'}{G} + \frac{\Omega}{2} \right), |V_{-S}| + |V_S| \ne 0$ and $G = G(\Xi)$ satisfies the equation

$$G'' + \Omega G' + \Psi G = 0, \tag{9}$$

where $V_i(\pm 1, \pm 2, ..., \pm S)$, Ω and Ψ are coefficient constants later. Implementing the homogeneous balance principle in equation (7), the positive integer S can be determined. From equation (5), we find that

$$\Delta = \tau - \Delta^2, \tag{10}$$

where $\tau = \dfrac{\Omega^2 - 4\Psi}{4}$ and τ is calculated by Ω and Ψ. So, Δ satisfies (10), which produces:

$$\Delta = \begin{cases} \dfrac{\sqrt{\Omega^2 - 4\Psi}}{2} \tanh\left(\dfrac{\sqrt{\Omega^2 - 4\Psi}}{2}\Xi\right), & \Omega^2 - 4\Psi > 0; \\ \dfrac{\sqrt{\Omega^2 - 4\Psi}}{2} \coth\left(\dfrac{\sqrt{\Omega^2 - 4\Psi}}{2}\Xi\right), & \Omega^2 - 4\Psi > 0; \\ \dfrac{1}{\Xi}, & \Omega^2 - 4\Psi = 0; \\ -\dfrac{\sqrt{\Omega^2 - 4\Psi}}{2} \tan\left(\dfrac{\sqrt{4\Psi - \Omega^2}}{2}\Xi\right), & \Omega^2 - 4\Psi < 0; \\ -\dfrac{\sqrt{\Omega^2 - 4\Psi}}{2} \cot\left(\dfrac{\sqrt{4\Psi - \Omega^2}}{2}\Xi\right), & \Omega^2 - 4\Psi < 0. \end{cases}$$

Family III: By implementing (9) and (8) and (7) and collecting all terms in the same order of Δ together, the left-hand side of (7) is converted into a polynomial in Δ. Equating each coefficient of the polynomial to zero, we can get a set of algebraic equations which can be solved to find the values of the studied method.

II.ii. Variation of $\left(G'/G\right)$-Expansion Method.

According to the the variation of (G'/G)-expansion method, we have

$$R(\Xi) = \sum_{i=0}^{M} R_i \mathrm{X}^i + \sum_{i=1}^{M} S_i \mathrm{X}^{i-1} \mathrm{Z}, \tag{11}$$

where $\mathrm{X} = (\Theta'/\Theta)$ and $\mathrm{Z} = (\omega'/\omega)$. and $\Theta = \Theta(\Xi)$ and $\omega = \omega(\Xi)$ represent the solution of the coupled Riccati equations

$$\Theta'(\Xi) = -\Theta(\Xi)\,\omega(\Xi), \qquad \omega'(\Xi) = 1 - \omega(\Xi)^2,$$

These coupled Riccati equations give us four types of hyperbolic function solutions including sech, tanh, csch and coth such as

$$\Theta(\Xi) = \pm \operatorname{sech}(\Xi), \qquad \omega(\Xi) = \tanh(\Xi),$$

$$\Theta(\Xi) = \pm \operatorname{csch}(\Xi), \qquad \omega(\xi) = \coth(\Xi).$$

Step 4: A polynomial in X or Z is accomplished by plugging equation (11) into equation (7). Determining the coefficients of the equivalent power of X or Z produces a system of algebraic equations, which can be determined to construct the values of R_i and S_i using MAPLE. Turning the over-measured values of R_i and S_i in 11, the general solutions of the studied equation complete the calculation of the result of the proposed model.

III. Fractional-order biological population model

We consider the proposed model:

$$\frac{\partial^\gamma Q}{\partial t^\gamma} - \frac{\partial^2}{\partial x^2}(Q^2) + \frac{\partial^2}{\partial y^2}(Q^2) + b(Q^2 - c) = 0, t > 0, 0 < \gamma \le 1 \tag{12}$$

Where Q denotes the population density, $b(Q^2 - c)$ represents the population supply due to births and deaths, b and c are constants and γ is a parameter describing the order of the fractional time derivative [4]. For our purpose, we introduce the following transformations:

$$Q(x, y, t) = Q(\Xi), \; \Xi = x + iy - \frac{a t^\gamma}{\Gamma(1+\gamma)}, \tag{13}$$

where a is a constant and $i^2 = -1$. From (13) and (12), we have:

$$a Q' + bQ^2 - bc = 0 \tag{14}$$

III.i. Fractional-order biological population model via modified $\left(G'/G\right)$– expansion method.

Now implementing the method of homogeneous balance between the highest order derivative and non-linear term in (14), then we find, $S = 1.$ According to the modified (G'/G)-expansion method, we get

$$Q = V_{-1}\Delta^{-1} + V_0 + V_1\Delta^1 \tag{15}$$

Substituting (15) into (14), collecting the coefficient of Δ and setting them to zero, then we find the following set of solutions:

Cluster I:

$$a = \frac{\pm 2b\sqrt{c}}{\sqrt{\Omega^2 - 4\Psi}},\ \ V_{-1} = 0,\ V_0 = 0,\ V_1 = \frac{\pm 2\sqrt{c}}{\sqrt{\Omega^2 - 4\Psi}}.$$

Substituting the values of Cluster I into (14), then we achieve :

$$Q_1(\Xi) = \pm\sqrt{c}\ \tanh\left(\frac{\sqrt{\Omega^2 - 4\Psi}}{2}\Xi\right). \tag{16}$$

$$Q_2(\Xi) = \pm\sqrt{c}\ \coth\left(\frac{\sqrt{\Omega^2 - 4\Psi}}{2}\Xi\right). \tag{17}$$

$$Q_3(\Xi) = \frac{\pm 2\sqrt{c}}{\sqrt{\Omega^2 - 4\psi}}\left(\frac{1}{\Xi}\right). \tag{18}$$

$$Q_4(\Xi) = \pm\sqrt{c}\ \tan\left(\frac{\sqrt{4\Psi - \Omega^2}}{2}\Xi\right). \tag{19}$$

$$Q_5(\Xi) = \pm\sqrt{c}\ \cot\left(\frac{\sqrt{4\Psi - \Omega^2}}{2}\Xi\right). \tag{20}$$

where $\Xi = x + iy - \dfrac{a t^{\gamma}}{\Gamma(1+\gamma)}$

Cluster II:

$$a = \frac{\pm b\sqrt{c}}{\sqrt{\Omega^2 - 4\Psi}},\ \ V_{-1} = 0,\ V_0 = \frac{\pm\sqrt{c}\sqrt{\Omega^2 - 4\Psi}}{4},\ V_1 = \frac{\pm\sqrt{c}}{\sqrt{\Omega^2 - 4\Psi}}.$$

Substituting the values of Cluster II into (14), then we achieve:

$$Q_6(\Xi) = \pm\left[\frac{\sqrt{c}\sqrt{\Omega^2 - 4\Psi}}{4} + \frac{\sqrt{c}}{2}\left\{\tanh\left(\frac{\sqrt{\Omega^2 - 4\Psi}}{2}\Xi\right)\right\}\right]. \tag{21}$$

$$Q_7(\Xi) = \pm\left[\frac{\sqrt{c}\sqrt{\Omega^2 - 4\Psi}}{4} + \frac{\sqrt{c}}{2}\left\{\coth\left(\frac{\sqrt{\Omega^2 - 4\Psi}}{2}\Xi\right)\right\}\right]. \tag{22}$$

$$Q_8(\Xi) = \pm\left\{\left(\frac{\sqrt{c}\sqrt{\Omega^2 - 4\Psi}}{4}\right) + \left(\frac{\sqrt{c}}{\sqrt{\Omega^2 - 4\Psi}}\right)\left(\frac{1}{\Xi}\right)\right\}. \tag{23}$$

$$Q_9(\Xi) = \pm\left[\frac{\sqrt{c}\sqrt{\Omega^2 - 4\Psi}}{4} - \frac{\sqrt{c}}{2}\left\{\tan\left(\frac{\sqrt{4\Psi - \Omega^2}}{2}\Xi\right)\right\}\right]. \tag{24}$$

$$Q_{10}(\Xi) = \pm\left[\frac{\sqrt{c}\sqrt{\Omega^2 - 4\Psi}}{4} - \frac{\sqrt{c}}{2}\left\{\cot\left(\frac{\sqrt{4\Psi - \Omega^2}}{2}\Xi\right)\right\}\right]. \tag{25}$$

Where $\Xi = x + iy - \dfrac{a t^{\gamma}}{\Gamma(1+\gamma)}$

Cluster III:

$$a=\frac{\pm 2b\sqrt{c}}{\sqrt{\Omega^2-4\Psi}},\ \ V_{-1}=\frac{\pm\sqrt{c}\sqrt{\Omega^2-4\Psi}}{2},\ V_0=0,\ V_1=0.$$

Substituting the values of Cluster III into (14), then we achieve:

$$Q_{11}(\Xi)=\pm\left[\frac{\sqrt{c}\,\sqrt{\Omega^2-4\Psi}}{2}\left\{\frac{\sqrt{\Omega^2-4\Psi}}{2}\tanh\left(\frac{\sqrt{\Omega^2-4\Psi}}{2}\Xi\right)\right\}^{-1}\right]. \tag{26}$$

$$Q_{12}(\Xi)=\pm\left[\frac{\sqrt{c}\,\sqrt{\Omega^2-4\Psi}}{2}\left\{\frac{\sqrt{\Omega^2-4\Psi}}{2}\coth\left(\frac{\sqrt{\Omega^2-4\Psi}}{2}\Xi\right)\right\}^{-1}\right]. \tag{27}$$

$$Q_{13}(\Xi)=\pm\left[\frac{\sqrt{c}\,\sqrt{\Omega^2-4\Psi}}{2}\left(\frac{1}{\Xi}\right)^{-1}\right]. \tag{28}$$

$$Q_{14}(\Xi)=\pm\left[\frac{\sqrt{c}\,\sqrt{\Omega^2-4\Psi}}{2}\left\{-\frac{\sqrt{\Omega^2-4\Psi}}{2}\tan\left(\frac{\sqrt{4\Psi-\Omega^2}}{2}\Xi\right)\right\}^{-1}\right]. \tag{29}$$

$$Q_{15}(\Xi)=\pm\left[\frac{\sqrt{c}\,\sqrt{\Omega^2-4\Psi}}{2}\left\{-\frac{\sqrt{\Omega^2-4\Psi}}{2}\cot\left(\frac{\sqrt{4\Psi-\Omega^2}}{2}\Xi\right)\right\}^{-1}\right]. \tag{30}$$

where $\Xi=x+iy-\dfrac{a\,t^{\gamma}}{\Gamma(1+\gamma)}$

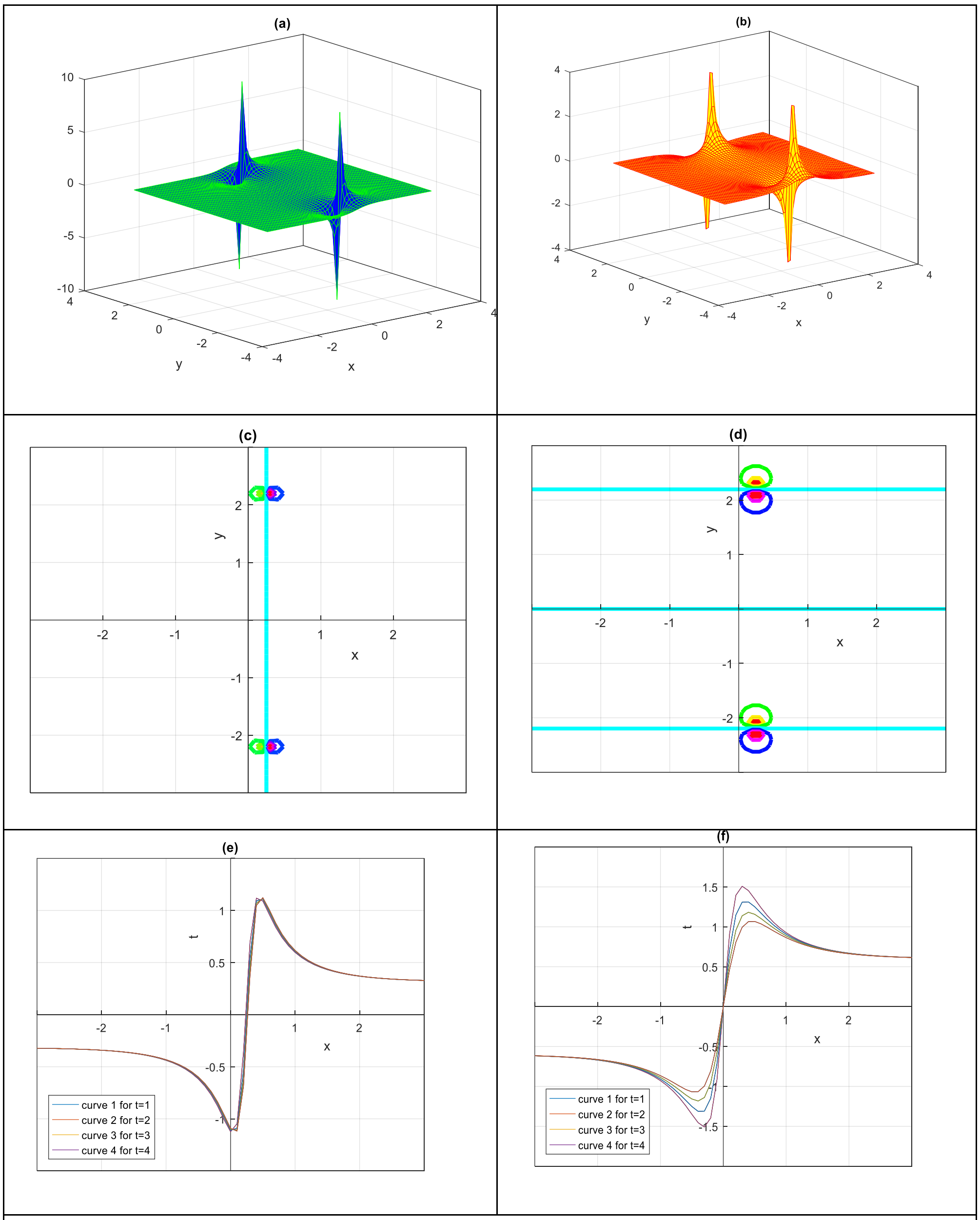

Fig. 1. The graphical representation of Eq.(16):(a) real 3D shape, (b) complex 3D shape,(c) real contour plot (d) complex contour plot, (e)real 2D shape, and (f) complex 2D shape.

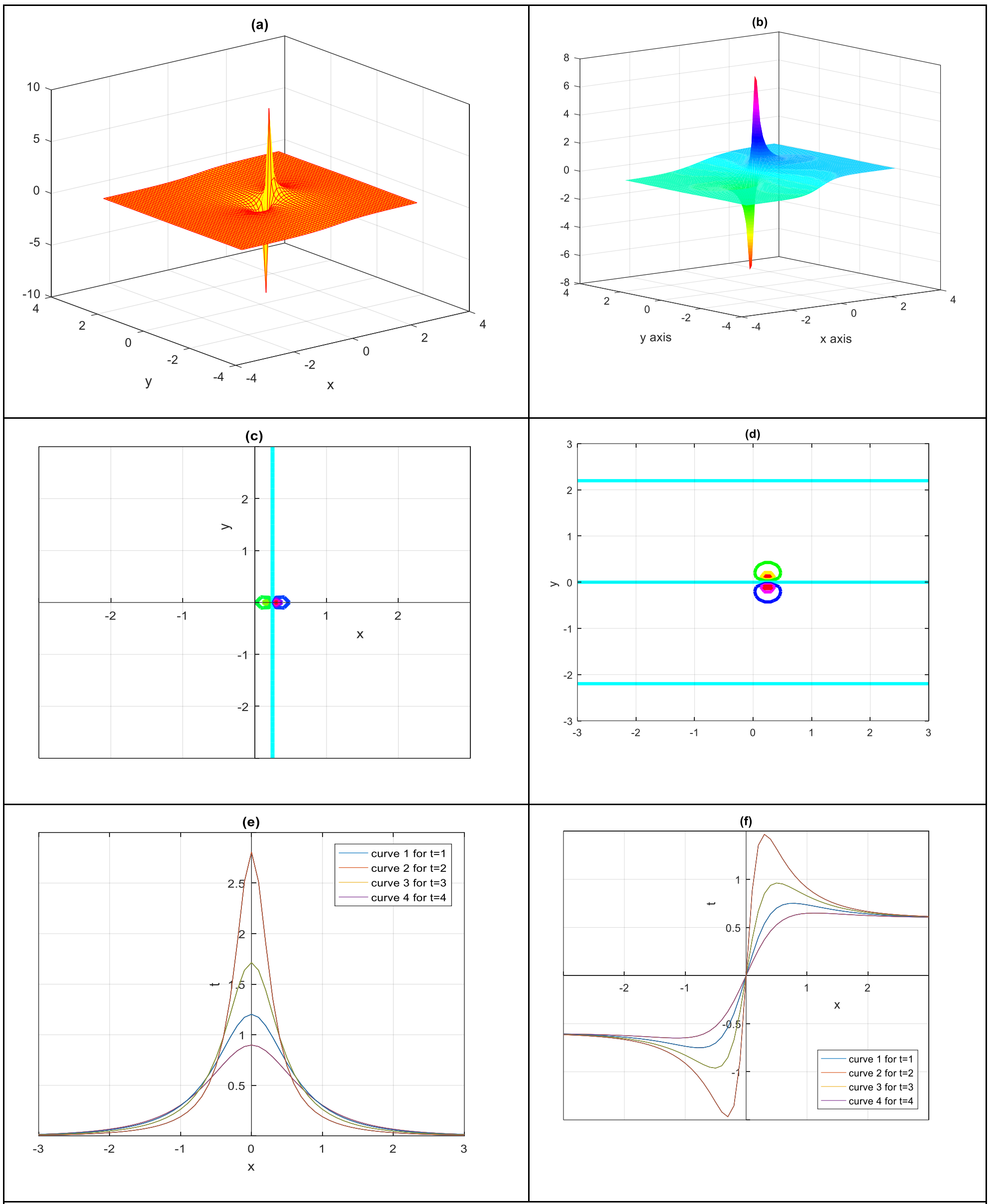

Fig. 2. The graphical representation of Eq.(17): (a) real 3D shape, (b) complex 3D shape,(c) real contour plot (d) complex contour plot, (e)real 2D shape, and (f) complex 2D shape.

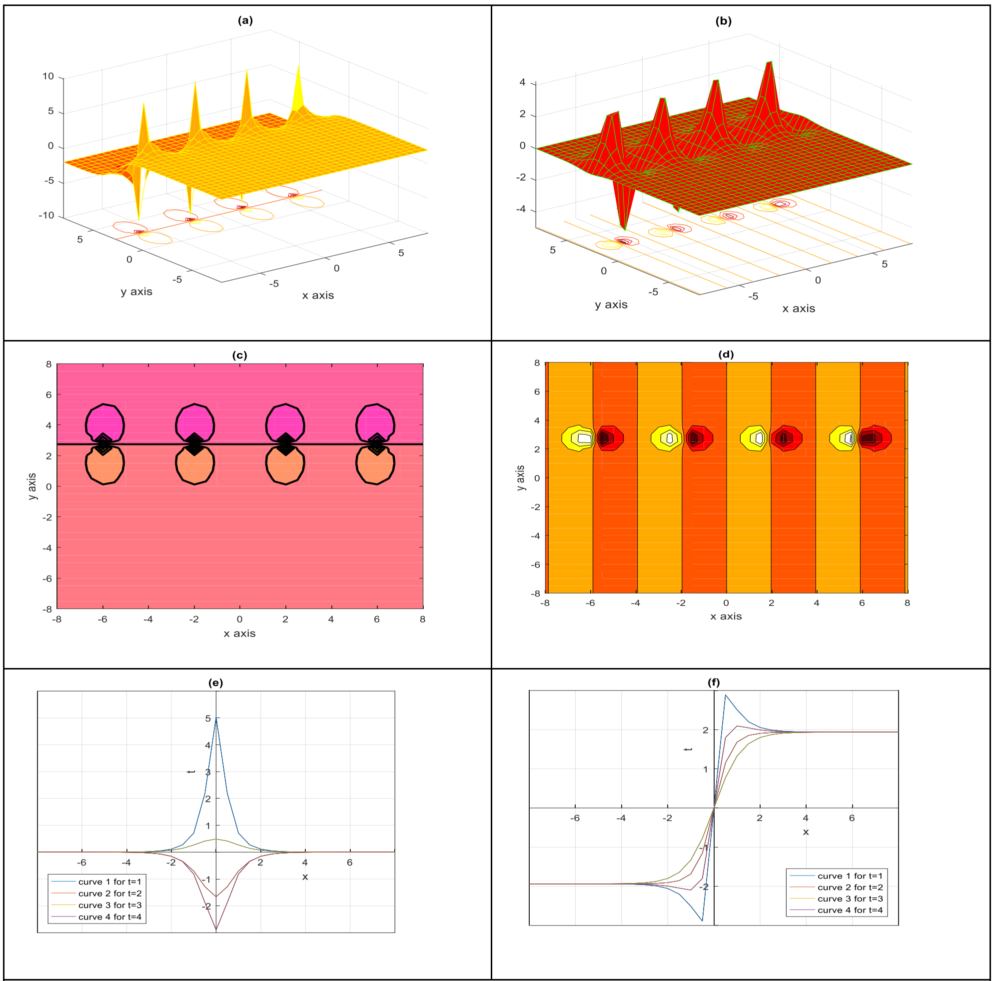

Fig. 3. The graphical representation of Eq.(19):(a) real 3D shape, (b) complex 3D shape,(c) real contour plot, (d) complex contour plot, (e) real 2D shape, and (f) complex 2D shape.

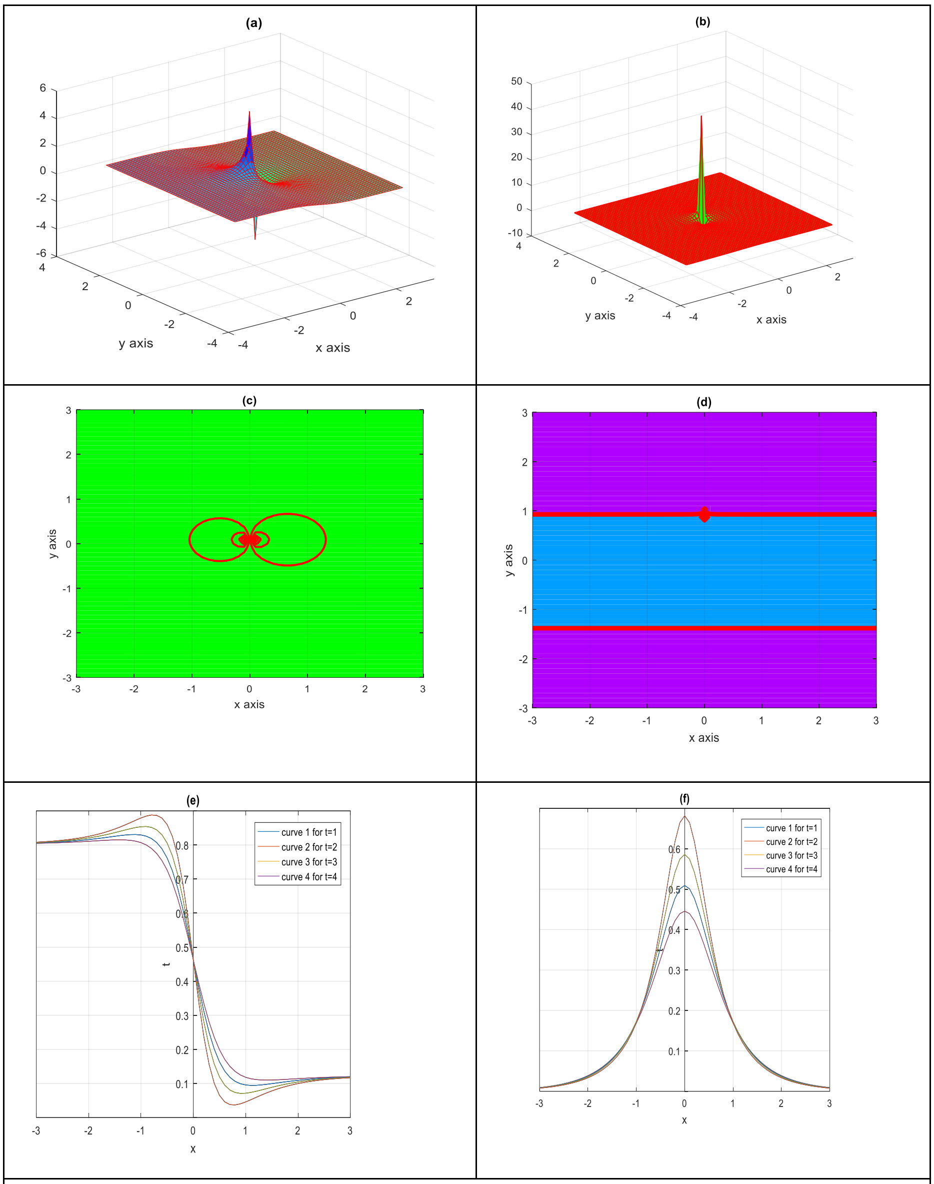

Fig. 4. The graphical representation of Eq.(22): (a) real 3D shape, (b) complex 3D shape,(c) real contour plot, (d) complex contour plot, (e) real 2D shape, and (f) complex 2D shape.

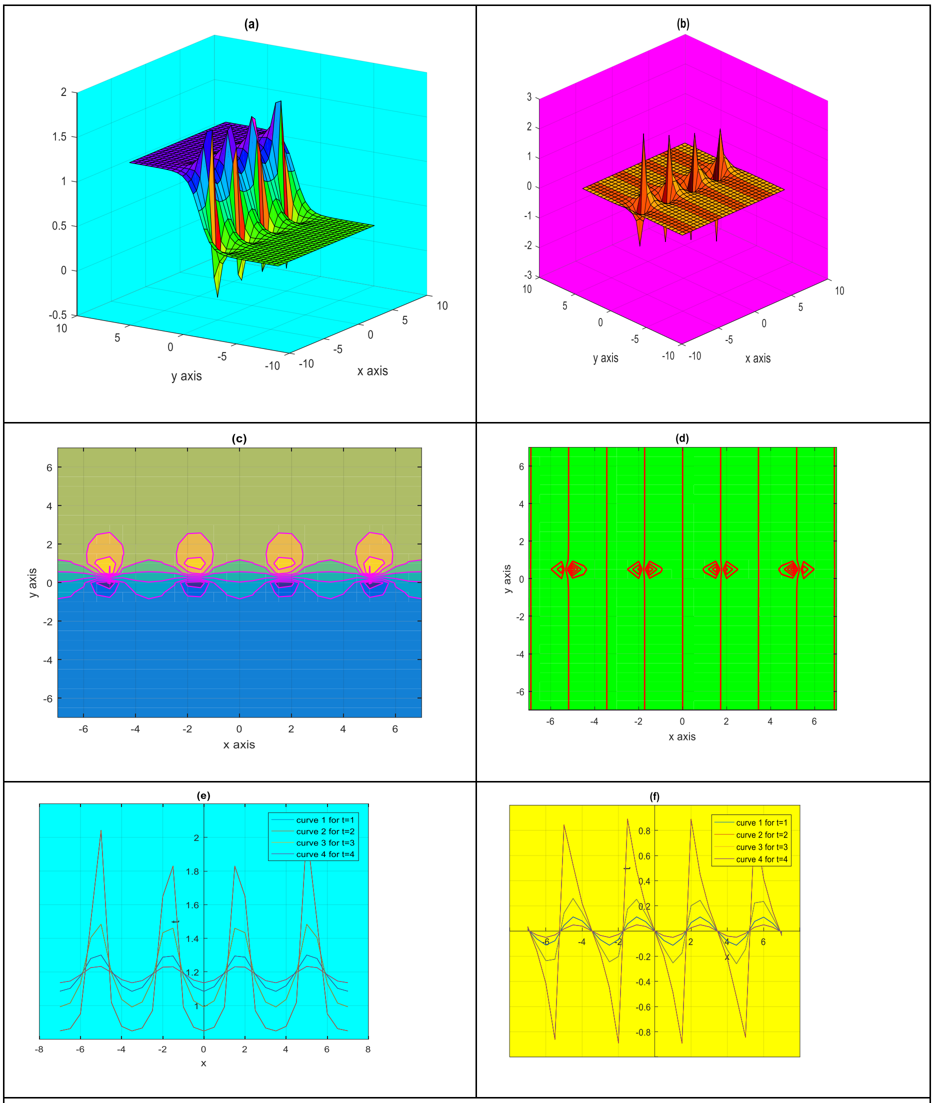

Fig. 5. The graphical representation of Eq.(24): (a) real 3D shape, (b) complex 3D shape,(c) real contour plot, (d) complex contour plot, (e) real 2D shape, and (f) complex 2D shape.

III.ii. Fractional-order biological population model via variation of $\left(G'/G\right)-$ expansion method.

Now implementing the method of homogeneous balance between highest order derivative and non-linear term in (14), then we find, $M=1$. According to the variation of $\left(G'/G\right)-$ expansion method, we get

$$Q(\Xi)=R_0+R_1\mathrm{X}+S_1Z=R_0+\frac{S_1}{\Theta}-(R_1+S_1)\Theta. \tag{31}$$

Substituting (31) into (14) and applying the necessary steps. Collecting the coefficient of X and Z solving the resultant system, then we find the following set of solutions:

Cluster I:

$$a = bW,\ R_O = 0,\ R_1 = \frac{-1}{\sqrt{W}} - \frac{c}{2W},\ S_1 = W,\ W = \left(-\frac{1}{4}c^2\right)^{\frac{1}{4}}$$

Substituting the above values in (31), we get:

$$Q_1(\Xi) = \frac{W}{\tanh(\Xi)} + \left(\frac{1}{\sqrt{W}} + \frac{c}{2W} + W\right)\tanh(\Xi). \tag{32}$$

$$Q_2(\Xi) = \frac{W}{\coth(\Xi)} + \left(\frac{1}{\sqrt{W}} + \frac{c}{2W} + W\right)\coth(\Xi). \tag{33}$$

Cluster II:

$$a = IbW,\ R_0 = 0,\ R_1 = -\frac{1}{\sqrt{W}} - \frac{c}{2WI},\ S_1 = IW,\ W = \left(-\frac{1}{4}c^2\right)^{\frac{1}{4}}$$

Substituting the above values in (31), we get:

$$Q_3(\Xi) = \frac{IW}{\tanh(\Xi)} + \left(\frac{1}{\sqrt{W}} + \frac{c}{2IW} + IW\right)\tanh(\Xi). \tag{34}$$

$$Q_4(\Xi) = \frac{IW}{\coth(\Xi)} + \left(\frac{1}{\sqrt{W}} + \frac{c}{2IW} + IW\right)\coth(\Xi). \tag{35}$$

Cluster III:

$$a = -bW,\ R_O = 0,\ R_1 = \frac{-1}{\sqrt{W}} + \frac{c}{2W},\ S_1 = -W,\quad W = \left(-\frac{1}{4}c^2\right)^{\frac{1}{4}}$$

Substituting the above values in (31), we get:

$$Q_5(\Xi) = \frac{-W}{\tanh(\Xi)} + \left(\frac{1}{\sqrt{W}} - \frac{c}{2W} + W\right)\tanh(\Xi). \tag{36}$$

$$Q_6(\Xi) = \frac{-W}{\coth(\Xi)} + \left(\frac{1}{\sqrt{W}} - \frac{c}{2W} + W\right)\coth(\Xi). \tag{37}$$

Cluster IV:

$$a = -IbW,\ R_O = 0,\ R_1 = \frac{-1}{\sqrt{W}} + \frac{c}{2IW},\ S_1 = -IW,\quad W = \left(-\frac{1}{4}c^2\right)^{\frac{1}{4}}$$

Substituting the above values in (31), we get:

$$Q_7(\Xi) = \frac{-IW}{\tanh(\Xi)} + \left(\frac{1}{\sqrt{W}} - \frac{c}{2IW} + IW\right)\tanh(\Xi). \tag{38}$$

$$Q_8(\Xi) = \frac{-IW}{\coth(\Xi)} + \left(\frac{1}{\sqrt{W}} - \frac{c}{2IW} + IW\right)\coth(\Xi). \tag{39}$$

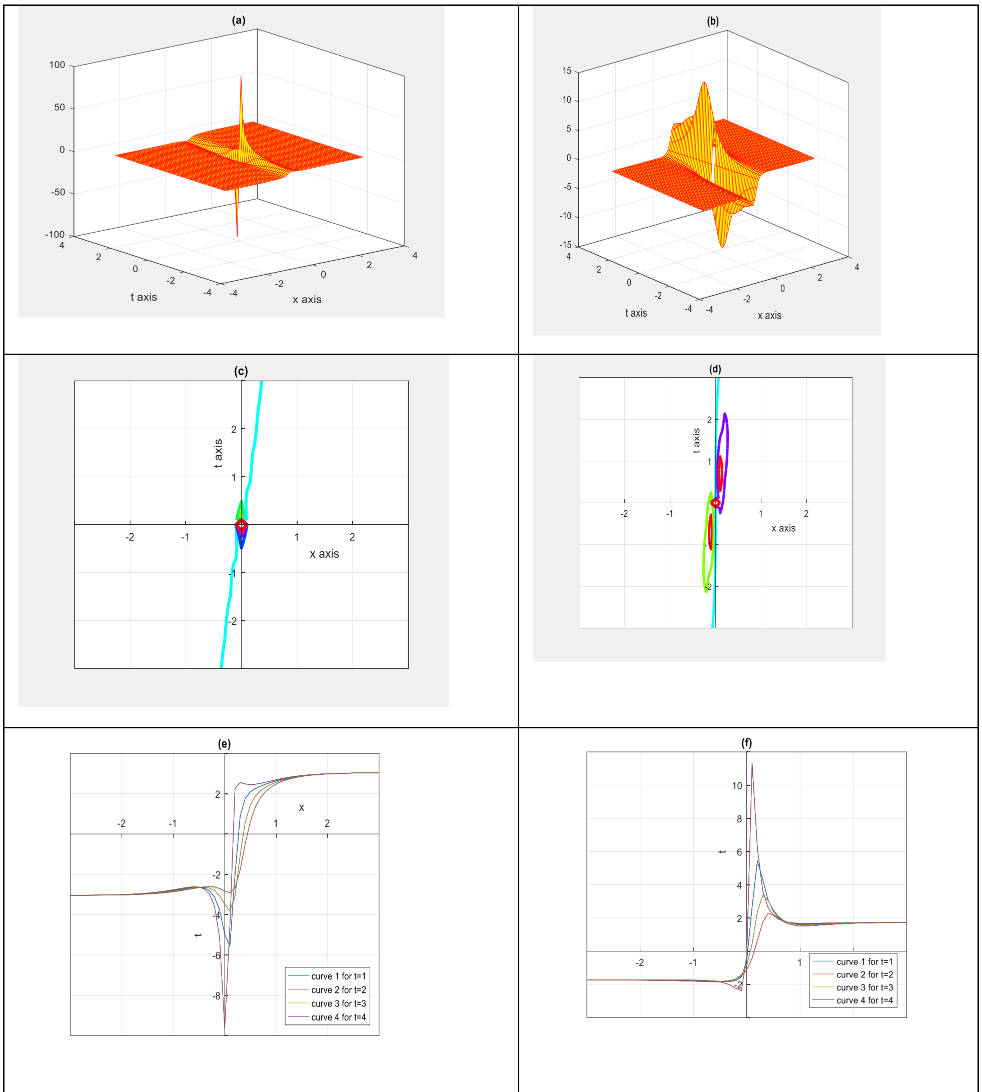

Fig. 6. The graphical representation of Eq.(32) :(a) real 3D shape, (b) complex 3D shape,(c) real contour plot, (d) complex contour plot, (e) real 2D shape, and (f) complex 2D shape.

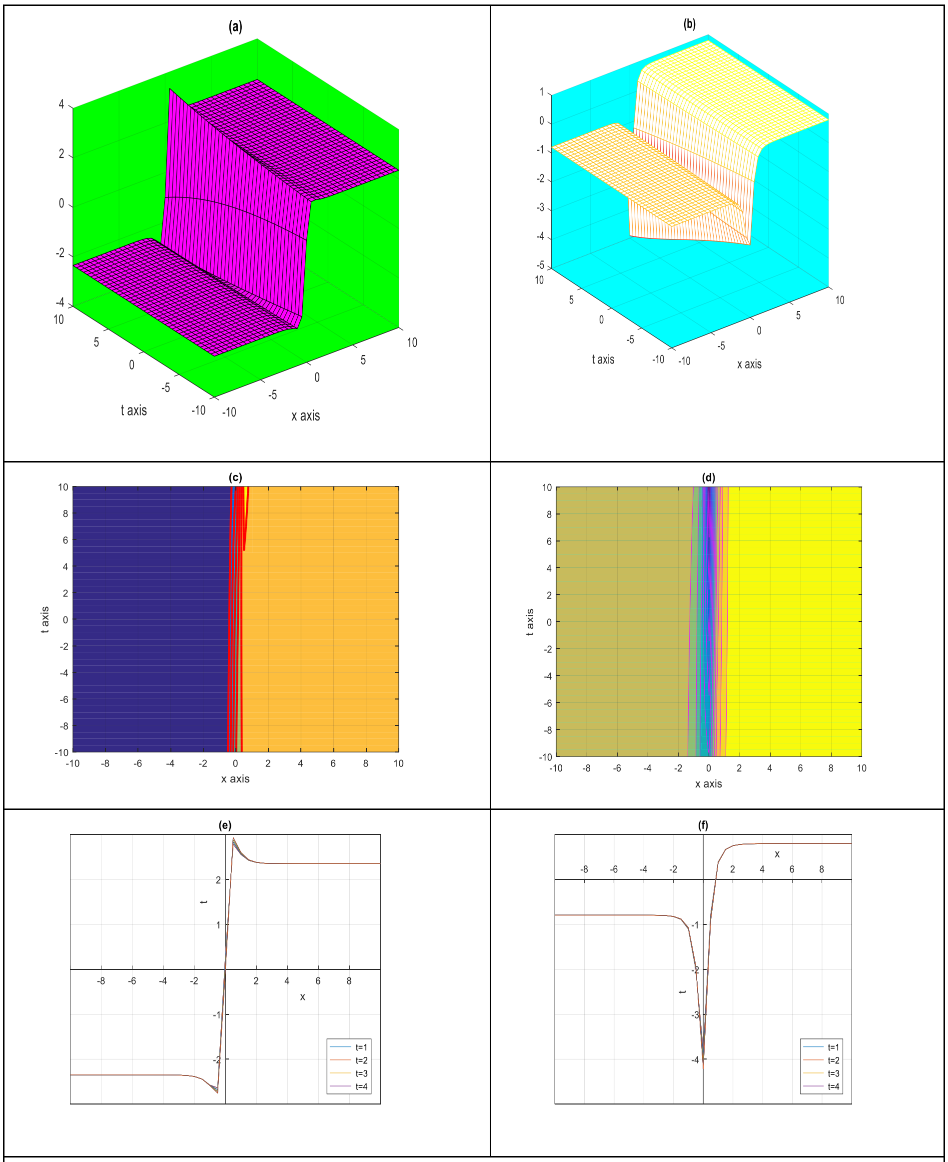

Fig. 7. The graphical representation of Eq.(32): (a) real 3D shape, (b) complex 3D shape, (c) real contour plot, (d) complex contour plot (e) real 2D shape, and (f) complex 2D shape.

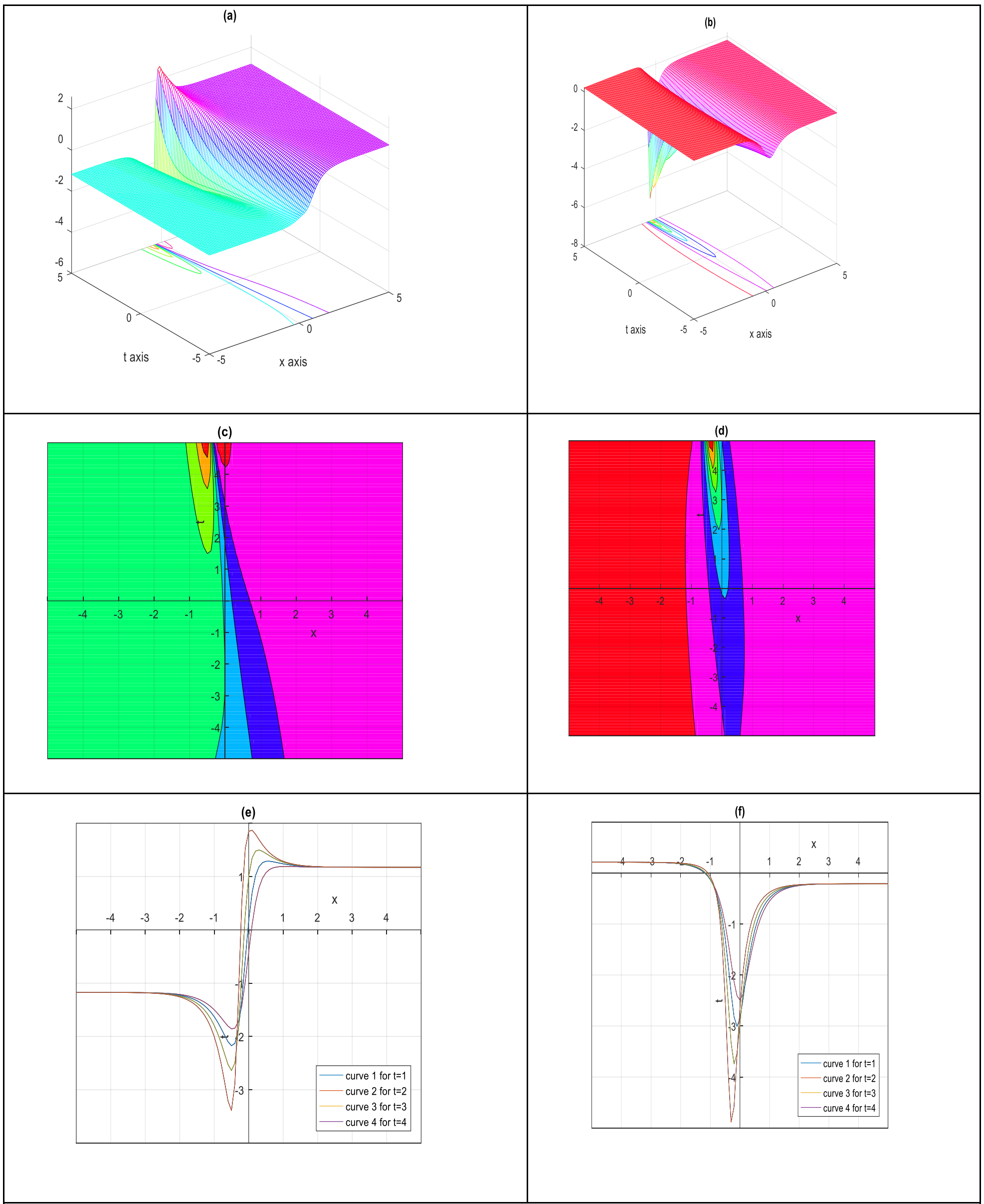

Fig. 8. The graphical representation of Eq.(34):(a) real 3D shape, (b) complex 3D shape, (c) real contour plot, (d) complex contour plot (e) real 2D shape and (f) complex 2D shape.

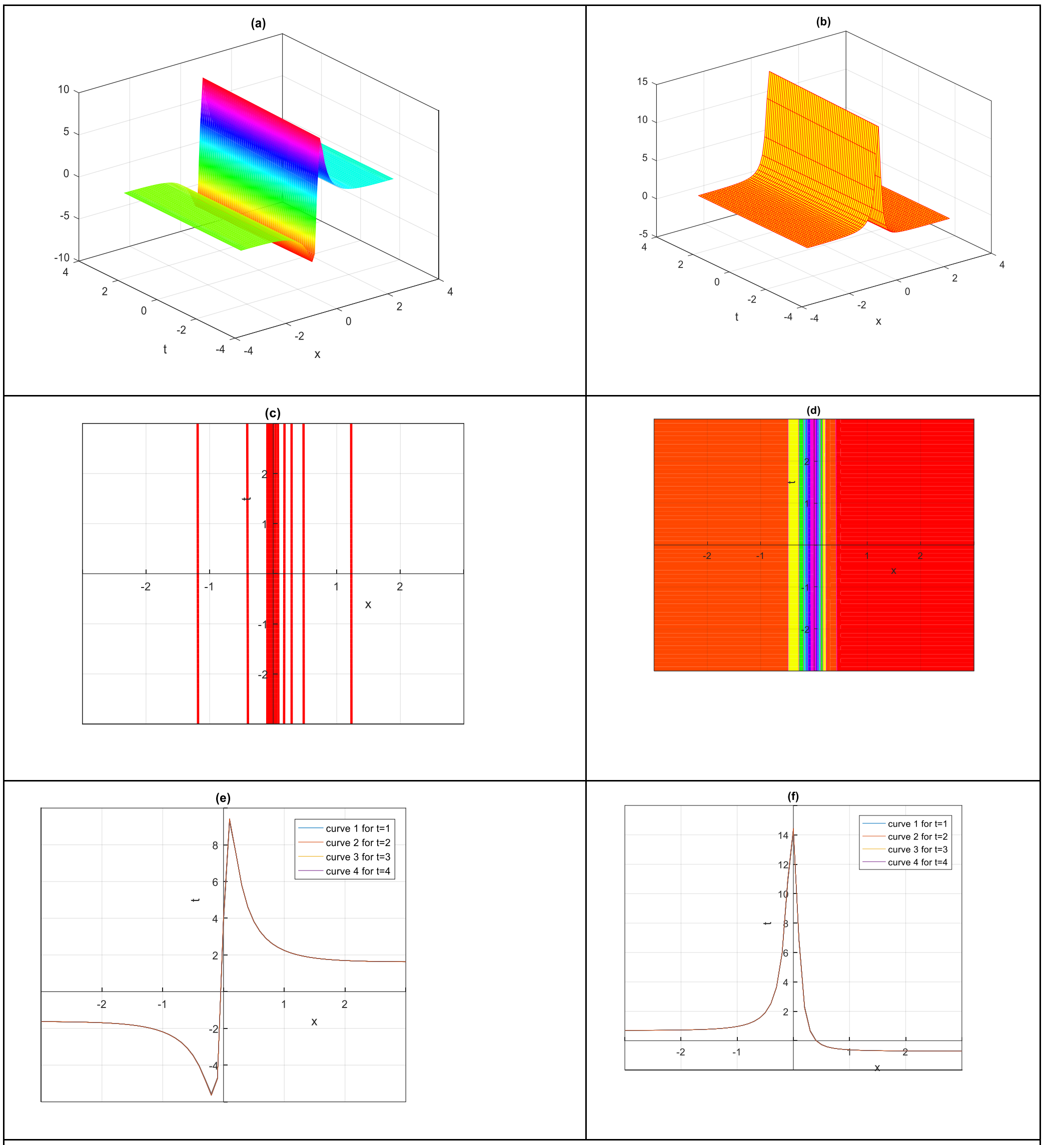

Fig. 9. The graphical representation of Eq.(37): (a) real 3D shape , (b) complex 3D shape , (c) real contour plot ,(d) complex contour plot (e) real 2D shape and (f) complex 2D shape.

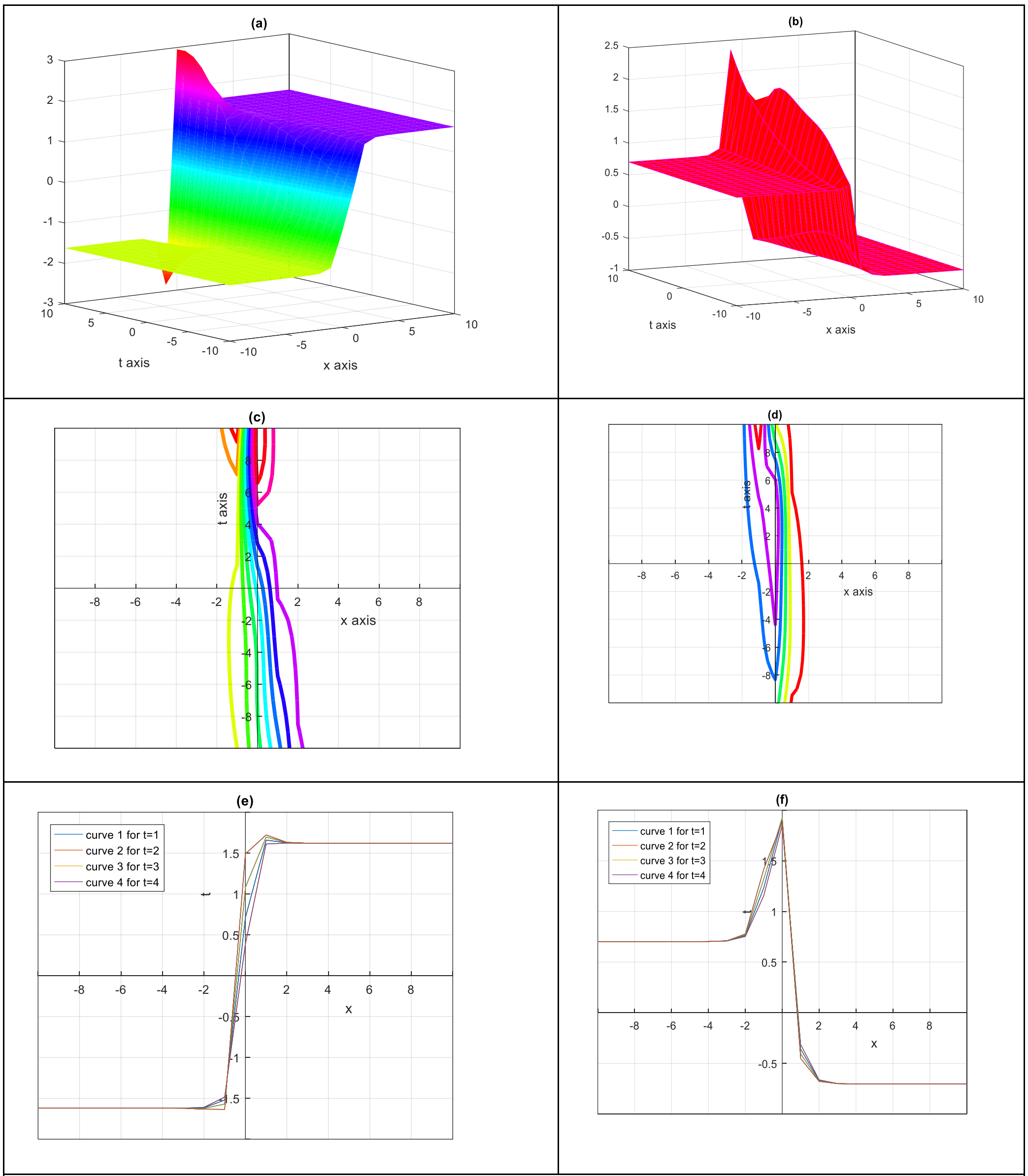

Fig. 10. The graphical representation of Eq.(37): (a) real 3D shape , (b) complex 3D shape , (c) real contour plot ,(d) complex contour plot (e) real 2D shape and (f) complex 2D shape.

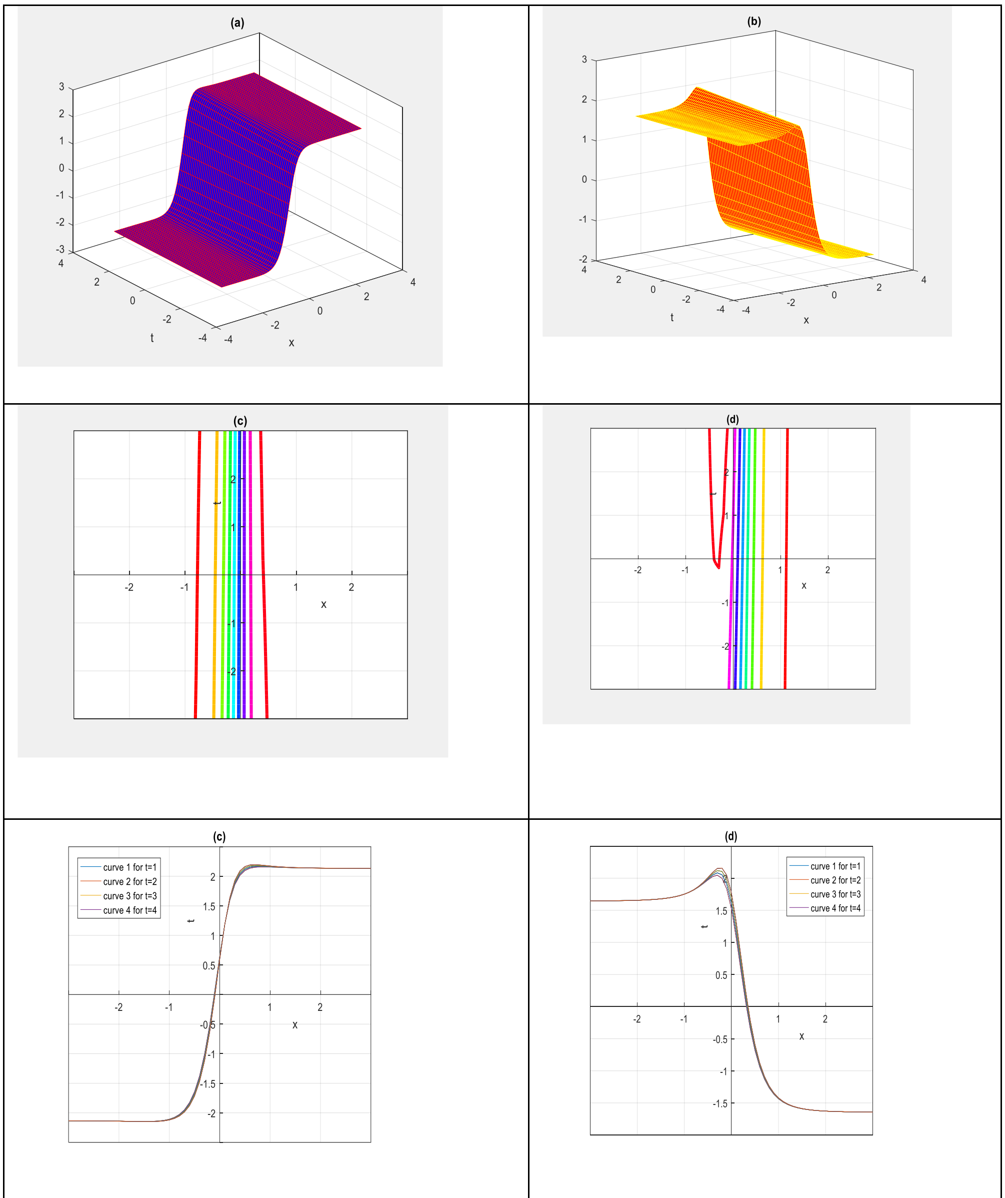

Fig. 11. The graphical representation of Eq.(38): (a) real 3D shape , (b) complex 3D shape , (c) real contour plot ,(d) complex contour plot (e) real 2D shape and (f) complex 2D shape.

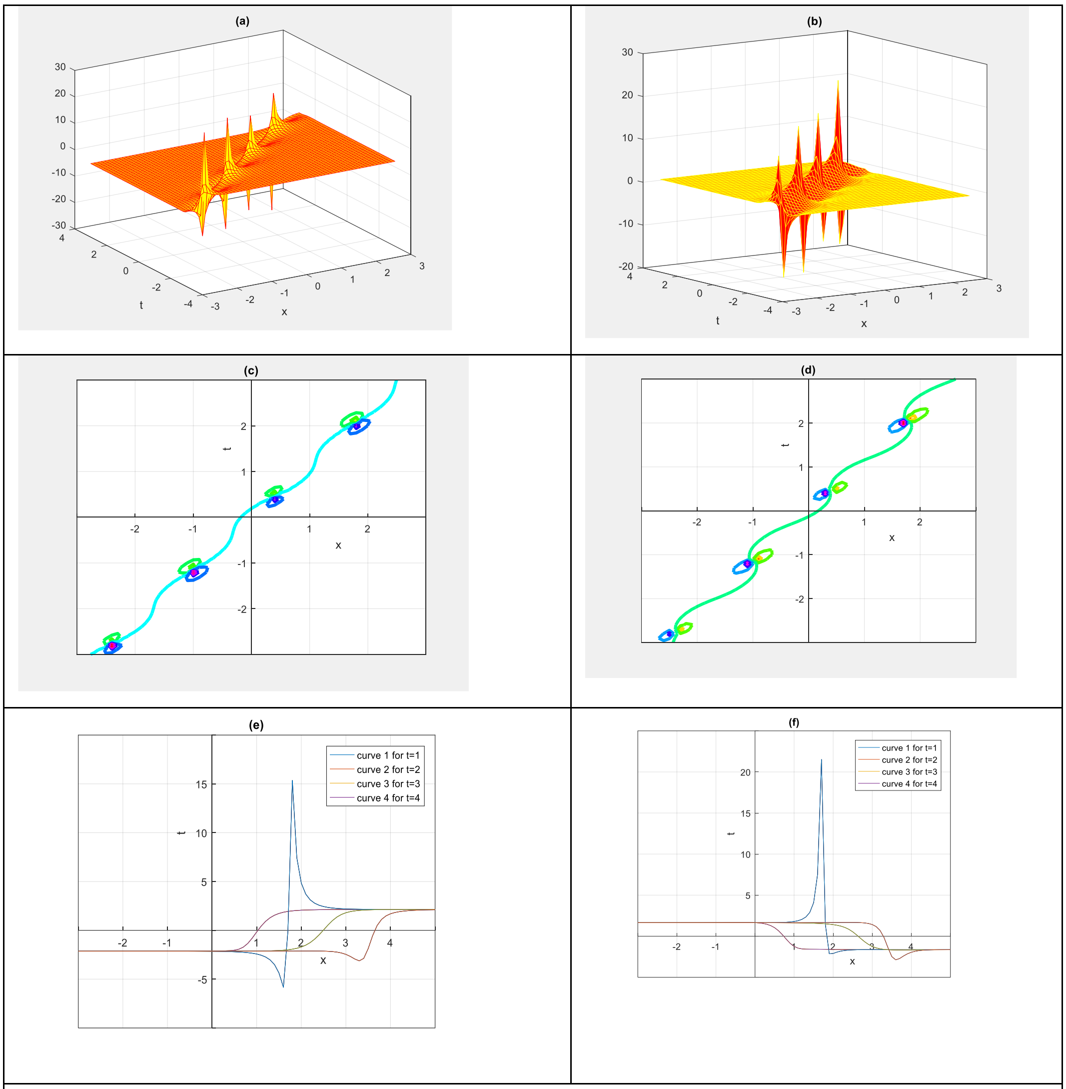

Fig. 12. The graphical representation of Eq.(39): (a) real 3D shape, (b) complex 3D shape, (c) real contour plot, (d) complex contour plot (e) real 2D shape, and (f) complex 2D shape.

IV. Numerical Simulations

In this portion, 23 new calculational outcomes are laid out, for example, trigonometric, hyperbolic, and rational determinations that addressed as king type, anti-king type, singular king, lump type, rogue type, the interaction of lump and rogue, multiple lump and rogue, interaction of lump and rogue with king solution, periodic lump, and rogue shape via our recommended techniques. A couple of graphical portrayals of the above-characterized new computational arrangements of the nonlinear fractional-order biological population model got using the proposed strategy have been given. Scarcely any picked computational outcomes will be portrayed as three-dimensional, two dimensional with different t and contour shapes.

Here, we partitioned the numerical simulation of two proposed techniques in the following two sections (4.1) and (4.2).

IV.i. Numerical Simulations via modified (G'/G)-expansion method

In the ongoing segment, we have offered various numerical simulations using the proposed approaches. To make sense of the powerful exhibitions of the responses procured in segment 3. Figures 1-5 show the graphical portrayals of a few chosen computational consequences of the issue got using the concentrated on strategy. They are presented underneath.

Figure 1 exhibits the unique presentation of Eq.(16)using the parameters $\Omega = 1.5, \Psi = 0.1, \gamma = 0.1.$ Specifically, Figure 1 shows the 3D form, 2D form, and contour form. Eq.(16). This shape addresses the multiple bright and dark lump wave profiles. The solution attributes of Eq.(17) are displayed in Figure 2 using $\Omega = 1.5, \Psi = 0.1, \gamma = 0.1.$ This shape addresses the single bright and dark lump wave profile. The nature of the result of Eq.(19) is shown in Figure 3 using $\Omega = 1, \Psi = 0.5, \gamma = 0.5.$This shape addresses the multiple periodic bright and dark lump wave profiles. In Figure 3 we also demonstrate the 2D and contour plot of Eq.(19). Figure 4 exhibits the unique presentation of Eq.(22) using the parameters $\Omega = 1.5, \Psi = 0.1, \gamma = 0.1.$ Specifically, Figure 4 shows the 3D form, 2D form and contour form of Eq.(22). This shape shows the single bright lump wave and single soliton wave profile. The solution of Eq.(24) are displayed in Figure 5 with 3D, 2D, and contour shapes which represents the intersection of multiple periodic lump and rogue wave profile for $\Omega = 1, \Psi = 1, \gamma = 0.1.$

IV.ii. Numerical Simulations via variation of (G'/G)-expansion method

In this part, we have introduced more than a couple of mathematical representations of the use of the proposed technique. To make consideration of the viable shows of the reactions secured in segment three. Figures 6-12 display the graphical depictions of a couple of chosen computational outcomes of the issue got utilizing the focused procedure. They are presented in descending.

Figure 6 exhibits the unique presentation of Eq.(32) using the parameters $b = 1, c = 2, y = 0, \gamma = 0.1.$ Specifically, Figure 6 shows the 3D form, 2D form, and contour form of Eq.(32). This shape tends to the single bright and dark lump wave profile as well as rogue wave profile. The solution of Eq. (32) $b = 2, c = 1, y = 2, \gamma = 0.01.$ represents the intersection of the king wave and multiple solitons which is illustrated in Figure 7. Figure 8 manifests the powerful execution of Eq.(34) using $b = 0.5, c = 0.2, y = 2, \gamma = 0.7.$ Specifically, Figure 8 illustrates the 3D figure, 2D figure, and contour figure of Eq.(34). This shape addresses the intersection of lump and kinky wave profile. Figure 9 manifests the powerful execution of Eq.(37) using $b = 0.5, c = 0.2, y = 3, \gamma = 0.007.$ Specifically, Figure 9 illustrates the 3D figure and contour figure of Eq.(37). This shape represents the lump, rogue, and soliton solution wave outline. Also, the solution of Eq.(37) demonstrates the intersection of the king and lump waveform $b=0.5, c=0.2, y=2, \gamma=0.5.$ which is displayed in Figure 10. The graphical representation of Eq.(38) describes the king and anti-king wave profile for $b=2, c=3, y=1, \gamma=0.005.$ exhibits in Figure 11. The solution of Eq.(39) for $b=2, c=3, y=1, \gamma=0.5.$ exposures to the periodic lump and rogue wave profile, is in Figure 12.

V. Conclusion

Our review has analyzed the new computational responses of the NFBP model by the proposed techniques. Various new computational outcomes have been accomplished in hyperbola, rational and trigonometric equations portrayed in king type shapes, singular king shapes, soliton solutions, singular lump and multiple lump shapes, periodic lump and rouge, the intersection of king and lump wave profile, the intersection of lump and rogue wave profiles. Contrasting our gained reactions and that acquired in recently composed research articles presents the uniqueness of our examination. The pre-owned technique's showcase uncovers that these strategies' adequacy and impact and their solidarity to carry out other nonlinear biological models merit future examination.

Conflict of Interest:

There was no relevant conflict of interest regarding this paper.

References

I. A. A. Kilbas, H. M. Sribastova, and J. J. Trujillo, Theory and Applications of Fractional Differential Equations, Elsevier, San Diego,2006.

II. A. Bekir ,'Application of the $\left(G'/G\right)-$expansion method for nonlinear evolution equations', Physics Letters A, vol. 372, pp, 3400–3406, 2008.

III. A. Khalid, A. Rehan, K. S. Nisar, and M. S. Osman,' Splines solutions of boundary value problems that arises in sculpturing electrical process of motors with two rotating mechanism circuit,' Physics Scripta, vol.96, no. 10, p. 104001, 2021.

IV. A. Korkmaz, O. E. Hepson, K. Hosseini, H. Rezazadeh and M.Eslami,' Sine-Gordon expansion method for exact solutions to conformal time fractional equations in RLW-class', Journal of King Saud University-Science, vol. 32,no.1, 2018.

V. A. R. Shehata and S. S. M. Abu-Amra,'Geometrical properties and exact solutions of the (3+1)-dimensional nonlinear evolution equations in mathematical physics using different expansion methods,'Journal of Advances in Mathematics and Computer Science, vol. 33, pp. 1-19, 2019.

VI. A. Zafar, M. Raheel, M. Q. Zafar et al.,'Dynamics of different nonlinearities to the perturbed nonlinear Schrodinger equation via solitary wave solutions with numerical simulations,'Fractal and Fractional, vol. 5, no. 4, p. 213, 2021.

VII. C. Park, R. I. Nuruddeen, K. K. Ali, L. Muhammad, M. S. Osman, and D. Baleanu,'Novel hyperbolic and exponential ansatz methods to the fractional fifth-order Korteweg de Vries equations,' Adv. Difference Equ., vol.2020, no. 1, p.627, 2020.

VIII. E. C. Ahsan and M. Inc,' Optical soliton solutions of the NLSE with quadratic-cubic-hamiltonian perturbations and modulation instability analysis', Optik, vol. 196,pp.162661 , 2019.

IX E. M. E.Zayed and K.A. Gepreel ,'The $\left(G'/G\right)-$ expansion method for finding traveling wave solutions of nonlinear partial differential equations in mathematical physics', Journal of Mathematical Physics, vol. 50 (1), pp, 013502, 2009.

X. G. Jumarie ,' Modified Riemann-Liouville derivative and fractional Taylor series of non-differentiable functions further results', Journal of Computer & Mathematics with Applications , vol. 51(9-10), pp, 1367-1376, 2006.

XI. G. Jumarie ,'Table of some basic fractional calculus formulae derived from a modified Riemann-Liouville derivative for non-differentiable functions', Journal of Applied Mathematics Letters , vol. 22(3), pp, 378-385, 2009.

XII. G. M. Ismail, H. R. A. Rahim, A. A. Aty, R. Kharabsheh, W. Alharbi and M. A. Aty,' An analytical solution for fractional oscillator in a resisting medium', Chaos, Solitons & Fractals, vol. 130,pp.109395 , 2020.

XIII. H. Ahmed, A. Akgul, T. A. Khan, P. S. Stanimirovic, and Y. M. Chu ,' A new analyzing technique for nonlinear time fractional Cauchy reaction-diffusion model equations,' Results in Physics' vol. 19,p.103462 , 2020.

XIV. H. Ahmed, A. Akgul, T. A. Khan, P. S. Stanimirovic, and Y. M. Chu ,' New perspective on the conventional solutions of the nonlinear time fractional partial differential equations,' Complexity' vol. 2020, Article ID 8829017, 10pages,2020.

XV. H. Yepez-Martinez and J. F.Gomez-Agular,‘ Fractonal sub-equation method for Hirota-Satsuma-coupled KdV equation and coupled mKdV equation using the Atangana’s conformable derivative’, Waves in Random and Complex Media , vol. 29,no.4, pp, 678–693, 2019.

XVI. I. Podlubny, Fractional Differential Equations, Academic Press, San Diego, 1999.

XVII. J. G. Liu, W. H. Zhu, M. S. Osman, and W. X. Ma,’An explicit plethora of different classes of interactive lump solutions for an extension form of 3D-Jimbo-Miwa model’, The European Physical Journal-Plus, vol. 135, no. 5, p. 412, 2020.

XVIII. K. Hosseini, M. Mirzazadeh, M. Ilie and S. Radmehr,‘ Dynamics of optical solitons in the perturbed Gerdjikov-Ivanov equation’, Optik, vol. 206,pp.164350 , 2020.

XIX. K. Hosseini, M. Mirzazadeh, J. Vahidi and R. Asghari,‘ Optical wave structures to the Fokas-Lenells equation’, Optik, vol. 207,pp.164450 , 2020.

XX. K. K. Ali, R. Yilmazer, and M. S. Osman,’Dynamic behavior of the (3+1)-dimensional KdV-Calogero-Bogoyavlenskii-Schiff equation,’Optical and Quantum Electronics, vol. 54, no. 3, p. 160, 2022.

XXI. K. S. Miller and B. Ross,’An introduction to the fractional calculus and fractional differential equations, Wiley, New York,1993.

XXII. M. N. Alam, A. R. Seadawy and D. Baleanu,‘Colsed-form wave structures of the space-time fractional Hirota-Satsuma coupled KdV equation with nonlinear physical phenomena,’ Open Physics, vol. 18,no.1,pp, 555–565, 2020.

XXIII. M. N. Alam, A. R. Seadawy and D. Baleanu,‘ Colsed-form wave solutions to the solitary wave equation in an unmaganatized dusty plasma’, Alexandria Engineering Journal , vol. 59,no.3, pp, 1505–1514, 2020.

XXIV. M. N. Alam and C. Tunc,‘The new solitary wave structures for the (2+1)-dimensional time fractional Schrodinger equation and the space-time nonlinear conformal fractional Bogoyav-lenskii equations,’ Alexandria Engineering Journal , vol. 59,no.4, pp, 2221–2232, 2020.

XXV. M. N. Alam, S. Aktar and C. Tunc,‘New solitary wave structures to time fractional biological population model ,’ Journal of Mathematical Analysis-JMA, vol. 11,no.3,pp, 59–70, 2020.

XXVI. M. N. Alam and X. Li,‘ New soliton solutions to the nonlinear complex fractional Schrodinger equation and conformal time-fractional Klein-Gordon equation with quadratic and cubic nonlinearity,’ Physics Scripta , vol. 95, no.4, pp, 045224, 2020.

XXVII. M. S. Osman, H. Rezazadeh and M. Eslami,'Traveling wave solutions for (3+1) dimensional conformal fractional Zakharov-Kuznetsov equation with power law nonlinearity', Nonlinear Engineering, vol. 8, no. 1, pp. 559-567, 2019.

XXVIII. M. Wang, X. Li and J. Zhang,'The $\left(G'/G\right)-$expansion method and travelling wave solutions of nonlinear evolution equation in mathematical physics', Physics Letters A, vol. 372(4), pp, 417–423, 2008.

XXXIX. S. Zhang and H. Q. Zhang,' Fractonal sub-equation method and its applications to the nonlinear fractional PDEs', Physics Letters A, vol. 375,no.7, pp, 1069–1073, 2011.

XXX. S. Zhang, J. L.Tong and W. Wang ,'A generalized $\left(G'/G\right)-$expansion method for the mKdv equation with variable coefficients', Physics Letters A, vol. 372, pp, 2254–2257, 2008.

XXXI. Z. B. Li and J. H. He ,'Fractional Complex Transform for Fractional Differential Equations', Journal of Mathematical and Computer Applications , vol. 15(5), pp, 970-973, 2010.

XXXII. Z. B. Li and J. H. He ,'Applications of the Fractional Complex Transformation to Fractional Differential Equations', Nonlinear science letters. A, Mathematics, physics and mechanics, 2, 121, 2011.